ACS APPLIED MATERIALS & INTERFACES

Research Article

www.acsami.org

Physics and Chemistry of Antimicrobial Behavior of Ion-Exchanged Silver in Glass

N. F. Borrelli,* W. Senaratne, Y. Wei, and O. Petzold

S&T Division, Sullivan Park, Corning Incorporated, Corning, New York 14830, United States

Supporting Information

ABSTRACT: The results of a comprehensive study involving the antimicrobial activity in a silver ion-exchanged glass are presented. The study includes the glass composition, the method of incorporating silver into the glass, the effective concentration of the silver available at the glass surface, and the effect of the ambient environment. A quantitative kinetic model that includes the above factors in predicting the antimicrobial activity is proposed. Finally, experimental data demonstrating antibacterial activity against *Staphylococcus aureus* with correlation to the predicted model is shown.

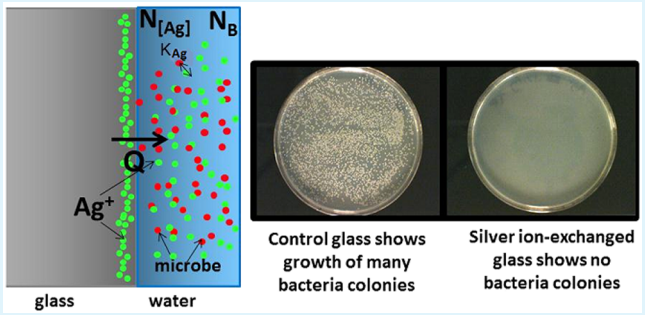

KEYWORDS: *antimicrobial, silver, ion-exchange, glass, relative humidity, mechanism*

1. INTRODUCTION

The ubiquitous use of smartphones and other hand-held devices has generated increased scientific and public concerns associated with bacteria on the surfaces of these devices. Implementing antimicrobial functionality on the surface of hand-held electronic devices, e.g., the cover glass of smartphones, is one approach to address the concerns via bacteria suppression. In this case one would first need to select the appropriate antimicrobial agent, and develop an understanding of how it is incorporated into the glass and how it is accessed to render the antimicrobial effect.

There has been extensive literature over the years up to the present dealing with the role of silver contained in various materials as an antimicrobial agent.[1−9] It is generally accepted that the Ag^+ ion is the antimicrobial agent, and in this study, the interest is in understanding the phenomenon as it occurs in the particular situation of silver-containing glasses. This study focus exclusively with the physical mechanism of the interaction as opposed to the actual biochemical process by which the silver disrupts the microbe causing death[10] and deals with the factors that might determine the efficacy of the antimicrobial (AM) action in terms of the disposition of the silver in the glass, as well as the influence of the ambient environment. In short, the interest is in the understanding of how the silver is released from the glass and brought into contact with the microbe, and how this Ag−microbe interaction can be optimized for AM activity. The following aspects will be studied and discussed in detail: (i) the glass composition, (ii) the method of incorporation of the silver into the glass, (iii) the effective concentration of the silver available at the surface (the use of "surface" is taken to mean the region where silver is available to participate in subsequent reactions), (iv) the effect of the ambient, and (v) an overall quantitative kinetic model predicting all the above factors for AM activity. A brief qualitative summary of these factors was given in a prior communication.[11] Finally, experimental data for *S. aureus* (Gram-positive bacteria) using a fairly stringent AM test protocol is shown with the relationship between the experimental and modeling data.

2. METHODS AND MATERIALS

2.1. Glass Composition. Experiments were carried out using alkali aluminoborosilicate glasses, such as Corning code 2318. As stated earlier, the effective species of silver is Ag^+. The role of the glass composition is to allow as much Ag^{1+} to be incorporated into the glass itself while maintaining the desired glass properties that are determined to a large extent by the specific glass product application.[12,13] In general, Ag^+ behaves in typical oxide glasses as a network modifier in a similar manner to Na^+ or K^+.[14−16] One approach to maximize the Ag^+ concentration is to melt a glass where silver is included as a salt in the batch formulation in a high concentration. Unfortunately, it is not that simple because, at high concentrations, Ag^+ has a propensity to reduce to the metal and the extent to which this happens is a function of the overall glass composition.[17,18] The reduced silver has two adverse effects: the first is that it reduces the amount of the active Ag^+, and the second is that it induces color in the glass which is not desired for certain applications.

A more efficient and less expensive way that uses less silver (since only the Ag^+ near the surface is involved in the AM activity) is to ion-exchange the Ag for the alkali using a Ag-containing molten salt bath,[19] after the glass formed into an

Received: May 16, 2014
Accepted: January 6, 2015
Published: January 6, 2015

DOI: 10.1021/am508159z
ACS Appl. Mater. Interfaces 2015, 7, 2195−2201

object (e.g., glass sheet). An example will be given below. It has the further advantages of (1) lessening the coloring effect, and (2) utilizing a variety of available commercial glasses which might have additional desirable thermomechanical properties. This is not to say that all commercial glass compositions are comparable in terms of good AM behavior, as will be pointed out with the in the discussion of other required properties.

2.2. Ion-Exchange Using (IOX) Ag Molten Salt Bath. Reagent grade salts $NaNO_3$, KNO_3, and $AgNO_3$ were used to prepare the molten baths. The baths were contained inside a furnace with temperature capability ranging from 300 to 450 °C. The temperature and time in the bath determined the diffusion depth, which can be predicted from the standard diffusion equation. $AgNO_3$/AlkaliNO_3 mixed baths were used rather than pure $AgNO_3$ for three reasons: the first is the cost, second is the stability against decomposition, and the third is greater control to achieve desired Ag^+ concentration (see section 3.2). The selection of the alkali bath to be used depends on the specific glass composition and whether it has been strengthened by ion exchange; this is in order to maintain the Ag as being the only diffusing species.

2.3. Characterization Techniques. There are a number of measurement techniques that were employed to characterize various aspects of the Ag disposition. For measurement of the depth of the ions after the ion-exchange, electron microprobe (EMP), X-ray photoluminescence spectroscopy (XPS), and secondary ion mass spectroscopy (SIMS) techniques were utilized. Inductively coupled plasma/mass spectroscopy (ICP/MS) was utilized to analyze the amount of Ag leached from the glass into a fixed amount of water for a given time. In addition, UV−vis spectroscopy was used to measure the relative amounts of Ag^{1+} in the glass from the shift in the UV absorption edge.

2.4. Glass Cleaning and Surface Preparation. All glass substrates were cleaned using a schedule consisting of a 4% Semiclean KG solution soak for 12 min at 70 °C in an ultrasound wash pulsed for 3 min and turned off for 3 min followed by a similar ultrasound rinse in DI water at 70 °C. The substrates were then dried in air at 80 °C. The substrates were stored in boxes prior to AM testing.

2.5. Antimicrobial Testing. Two tests were used to evaluate the antimicrobial efficacy. The first is the JIS Z 2801:2010 published by the Japanese standards association for antimicrobial products, *Test for Antimicrobial Activity and Efficacy*.[20] The second test is a modified test based on the EPA approved protocol for copper surface, *Test Method for Efficacy of Copper Alloy Surfaces as a Sanitizer*. JIS Z test is run as a covered test which makes it relatively independent of the ambient. The second test was developed for AM efficacy of copper metal, but with some modifications converted to a more generally applicable test for silver containing glasses. This test is perceived to be more stringent since the sample is left open to the ambient conditions and, therefore, is very sensitive to temperature and relative humidity. Details of these tests, the bacteria used, and the log reduction calculations are described in the Supporting Information.[21,22]

Reports in the literature of antimicrobial activity of Ag and other agents often are widely varied in their tests thus making reproducibility difficult. This paper shows antibacterial results based on the more stringent test. Results for the JIS Z are discussed in detail elsewhere.[13]

3. RESULTS AND DISCUSSION

3.1. Measurement of the Ag^{1+} Concentration Profile. As mentioned above, the antibacterial action produced by the silver ions is a "surface effect". Therefore, a quantitative knowledge of the surface Ag^{1+} concentration, in $\mu g/cm^2$ or ions/cm^2, is critical in ascertaining the effectiveness of the antimicrobial action. Silver in the body of the glass below the surface plays no antimicrobial role since it has no access to the bacteria on the surface. This is even more pertinent in the present case where the Ag is being added by an ion-exchange process. The analytical techniques of EMP, XPS, and SIMS were used to obtain the Ag^{1+} profile, but they yield volume concentration values, albeit close to the surface, whereas what is important is the surface ion concentration. Figure 1 is a graph

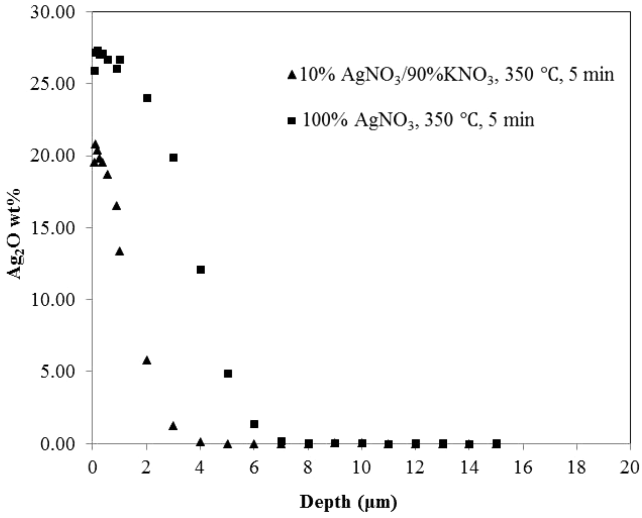

Figure 1. EMP profiles after Ag ion exchange using two different bath concentrations, exchange time was 5 min at 350 °C.

of EMP results showing the silver ion concentration, expressed as Ag_2O wt %, versus depth for glass samples that were prepared from a 10 wt % $AgNO_3$/90 wt % KNO_3 and 100 wt % $AgNO_3$ bath on IOX strengthened Corning glass code 2318.

Table 1 gives the Ag^+ bath concentrations, the time for ion-exchange, and the resulting EMP measurements (at 50 nm depth), as wt % Ag_2O, for several different ion-exchanges for IOX strengthened Corning glass code 2318. The number term "EMP (≅50 nm)" refers to a depth which is as close as the

Table 1. Ag Ion Bath Concentrations, the Time for Ion-Exchange at 350 °C, and EMP Measurements at 50 nm Depth

$AgNO_3$ wt % in bath	IOX time, min	EMP (≅50 nm), wt %[a]
0.15	20	0.82
0.15	330 (5.5 h)	1.0
0.25	20	1.0
0.5	20	2.2
1.0	20	5−7
2.0	20	7.1−8.1
5.0	20	12.3−15.3
10.0	10	23−25
50.0	5	28−30
100	5	28−30

[a]wt % was calculated as the oxide, Ag_2O.

DOI: 10.1021/am508159z
ACS Appl. Mater. Interfaces 2015, 7, 2195−2201

EMP method allows. The ion-exchange was done using a mixed $AgNO_3/KNO_3$ or 100 wt % $AgNO_3$ bath as noted in Table 1.

3.2. Model for Concentration of Ag in Glass Obtained from Ion-Exchange Bath. As shown below, the relationship of the steady-state concentration of Ag^+ in the molten bath (e.g., $xAgNO_3$ $(1-x)$ MNO_3, M being an alkali) to that in the glass is not a straightforward one. It is both glass composition and bath composition dependent, that is, whether the ion-exchange of Ag is for Li, Na, or K. A brief review of the statistical mechanical approach used by Araujo is needed to explain the ion exchange mechanism.[15] The reader is referred to the original article for the actual derivation.

Araujo utilizes a statistical mechanical model for the chemical potentials of the two mobile ions, A and B, both in the glass and the bath for the reaction given below.

$$A_{bath} + B_{glass} \Leftrightarrow A_{glass} + B_{bath} \quad (1)$$

The computed chemical potentials for the respective constituents are used to derive the equilibrium curves relating the mole fraction of the two respective phases. The basis for the analysis can be stated in the following equation where A and B represent the two exchanging mobile ions, in the bath and in the glass

$$(\mu_A - \mu_B)_{glass} = (\mu_A - \mu_B)_{bath} \quad (2)$$

and where μ represents chemical potential of either species in either phase defined as

$$\mu_i = \frac{-\partial(kT \ln Q)}{\partial N_i} \quad (3)$$

Here, Q is the statistical mechanical partition function, and N is the total number of species. The reader is referred to the original paper for the detailed expressions according to eq 1. With considerable algebra and some simplifying assumptions the analysis reduces to a two parameter model, one being the magnitude and sign of the A−B ion interaction energy term "E" and the other relating the mole fractions $X_A = N_A/(N_A + N_B)$ and $X_B = N_B/(N_A + N_B)$, with N being the molar concentration of each component in the glass, to the mole fraction in the bath defined by the following;

$$K_{eq} = a_A^{glass} a_B^{bath} / a_A^{bath} a_B^{glass} = \frac{(\gamma_A^{glass} X_{Aglass})(\gamma_B^{bath} X_{Bbath})}{(\gamma_A^{bath} X_{Abath})(\gamma_B^{glass} X_{Bglass})} \quad (4)$$

Here, the γ notation represents activity coefficients.

There is a closed form solution to this expression for the mole fraction of Ag in the glass of the form shown in eq 5

$$X_{Aglass} = \left(\frac{1 \pm \left[\frac{Rp - R}{Rp - 1} \right]^{1/2}}{2} \right) \quad (5)$$

Here the two fitting parameters E and K_{eq} are contained in the following expressions relating to eq 5.

$$R = [(K' - 1)/(K' + 1)]^2$$

$$K' = K_{eq}(1 - X_{Abath})/X_{Abath}$$

$$p = 1 - \exp(E/kT)$$

Equation 5 is used to calculate the Ag^+ fraction in the glass (X_{Aglass}) as a function of the molar fraction of the Ag^+ in the bath (X_{Abath}) with the E and K_{eq} parameters. These are shown in Figure 2 for a typical alkali aluminoborosilicate glass. A series

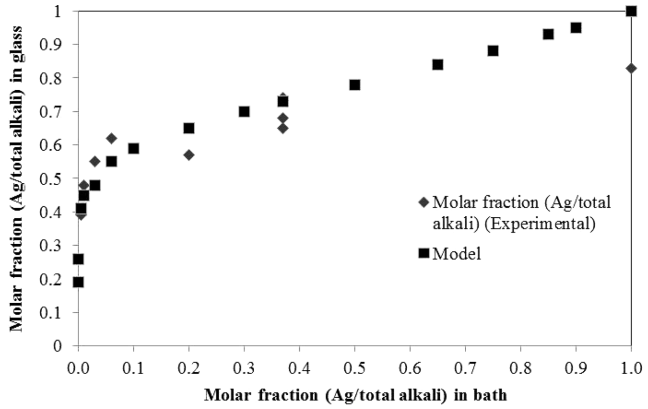

Figure 2. Model prediction of the Ag in glass as a function of the Ag in the bath for a typical alkali aluminoborosilicate glass (model parameters $E = -3$, $K_{eq} = 0.025$).

of $AgNO_3/KNO_3$ baths at various fractions were prepared, and the IOX glass samples were exposed to the baths for times of either of 5 or 10 min at a set temperature of 350 °C. EMP values from Table 1 were used and converted to molar fraction of (Ag/total alkali) in the bath, to determine the molar fraction of (Ag/total alkali) in the glass at a depth of 50 nm, which is taken to a reasonable approximation to the actual concentration near the glass surface.

One can see that the relationship of the Ag in the glass to that in the molten bath is highly nonlinear. It also should be pointed out that the shape of the curve is dependent on the specific glass composition because the activity coefficients are a function of the specific glass composition.

3.3. Role of Hydrated Layer. To interpret antimicrobial behavior one needs to understand the role of the ambient. It is obvious that any reaction of the microbe with the Ag^+ occurs on the surface and that there must be a liquid vehicle to support the Ag^+ and the microbe. This vehicle is the ubiquitous hydrated layer as discussed in several references as the hydrogen bonded (chemically adsorbed) and physisorbed water layers.[23,24]

One study[25] uses an IR measurement of the water on a glass surface in a cell with controlled relative humidity (RH) to measure the water layer thickness (number of water layers) as a function of the relative humidity. The results taken from the paper are shown in Figure 3.

A model is proposed that asserts water in the form of moisture on the surface equilibrated from the ambient air provides the mediating role as the support vehicle. A further assumption is that the Ag^{1+} near or at the glass surface comes into equilibrium with that in the hydrated layer via ion exchange of H^+ or H_3O^+ in the hydrated layer for Ag^+, (referred to as "leaching"), where the interaction with the bacteria occurs. A simple cartoon shown in Figure 4 shows the proposed situation.

The following experiment was to estimate how much Ag^+ from the glass equilibrates with that in the hydrated layer. Experimentally, as a surrogate we used a "leaching" approach where duplicates of the Ag^+-containing glass were soaked in DI

DOI: 10.1021/am508159z
ACS Appl. Mater. Interfaces 2015, 7, 2195−2201

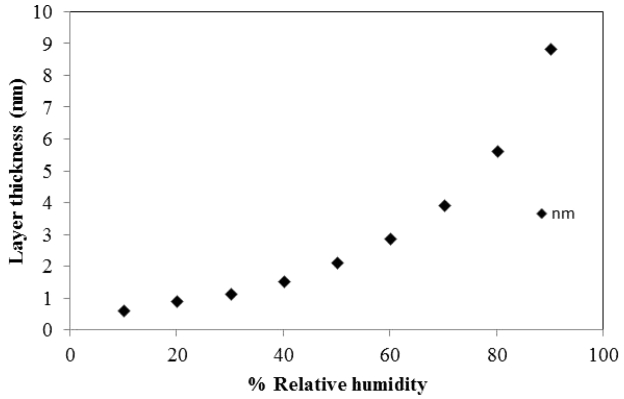

Figure 3. Thickness of hydrated layer as a function of RH; data replotted from ref 25.

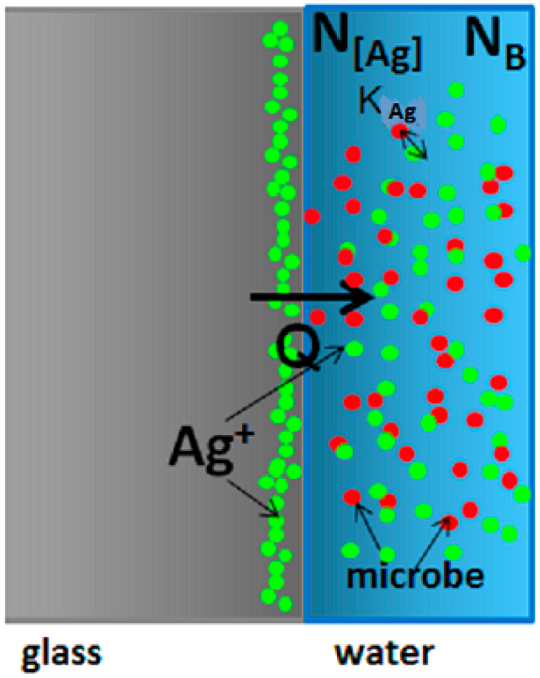

Figure 4. Schematic representation of the interaction of the Ag^+ in the hydrated layer with the microbe (Q, K_{Ag}, N_{Ag}, and N_B definitions are in Table 3).

water for 2−8 h and then measured the amount of Ag in the leach solution using ICP/MS detection. This method is able to quantitatively measure Ag in the ppb level. Table 2 shows the molar fraction of silver in solution determined from the leached silver using the ICP/MS data.

One now has recourse to the Araujo chemical potential model[15] where now one considers the "bath" as the Ag-containing glass and the "glass" now in this application constitutes the hydrated layer. In Figure 5, the calculation of using this model, to obtain molar fraction of Ag in solution as a function of the molar fraction (Ag/total alkali) in glass, is shown. An agreement with experimental leaching data for various bath concentrations that is listed in Table 2 is shown.

Table 2. Molar Fraction of Silver in the Leached Solution for Various $AgNO_3/KNO_3$ wt % Bath Concentrations

wt % $AgNO_3$ in bath	molar fraction of silver in solution (av)
5	$1.46 \times 10^{-09} \pm 5 \times 10^{-10}$
10	$1.58 \times 10^{-09} \pm 2 \times 10^{-10}$
20	$1.36 \times 10^{-09} \pm 1 \times 10^{-10}$
50	$1.64 \times 10^{-09} \pm 1.9 \times 10^{-10}$
100	$3.15 \times 10^{-09} \pm 1.2 \times 10^{-10}$

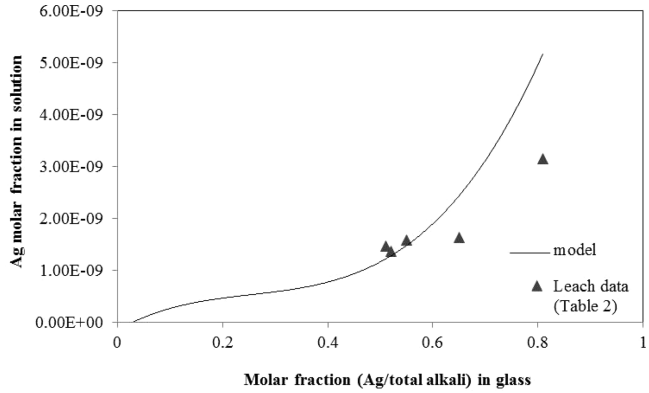

Figure 5. Model fit to Ag/total alkali in glass molar fraction to molar fraction in hydrated layer with model parameters E/kT = +2.3 and $K_{eq} = 8 \times 10^{-7}$. Experimental data points from Table 2 are plotted to show agreement.

Although the Ag^+ in the leached solution is not numerically equal to what would be in the hydrated layer, it should be proportional, so that this can be used as a surrogate in modeling in the next section, for the kinetic model. In other words one of the inputs to the subsequently derived "kinetic" model is the concentration of the Ag^+ in the hydrated layer. This value can be scaled, so relevance is not the absolute value itself but how it changes with Ag in the glass.

3.4. Kinetic Model. Finally, a general kinetic model is proposed which can be used to better understand the AM results irrespective of the type of test that is used, in particular the role of the ambient humidity. The proposed model asserts that interaction of the Ag^+ with the microbe all happens in the hydrated layer where both species are sufficiently mobile so that diffusion can be ignored, although one could easily add the terms if required.

Rate equations are expressed in eqs 6 and 7 below. The first quasidiffusion term expresses the rate at which the Ag^+ is moving into the hydrated layer from the glass; here, Ag_0 is the amount of Ag available in the glass, and N_{Ag} represents the total amount of Ag^+ in the volume (V) of liquid. That is, $N_{Ag} = V[Ag^+]$. Since the experiments deal with a constant surface area, one can write $V[Ag^+] = AT[Ag^+]$, where T is the thickness of the fluid layer, $[Ag^+]$ is the maximum concentration of silver ions in the hydrated layer, and A is the surface area of the glass. N_B represents the total number of bacteria in the layer at any given time. Equation 7 relates the bacteria content at any time t. The first term, $k_B N_B$, represents any bacteria, growth or death, during the time of the exposure other than the reaction with the silver, and the second term represents the interaction of bacteria with silver in the hydrated layer.

$$\frac{dN_{Ag}(t)}{dt} = Q\,Ag_0[T[Ag^+] - N_{Ag}(t)] - K_{Ag}N_{Ag}(t)N_B(t) \quad (6)$$

$$\frac{dN_B(t)}{dt} = k_B N_B - K_{Ag}N_{Ag}(t)N_B(t) \quad (7)$$

DOI: 10.1021/am508159z
ACS Appl. Mater. Interfaces 2015, 7, 2195−2201

Table 3 gives a complete definition of terms. Now, one can see how the thickness of the water layer allows more Ag^{1+} to be made available through the $T[Ag^+]$ term in eq 6, which is related to the discussion of the role of the hydrated layer discussed above and ultimately to the AM property discussed next.

Table 3. Definition of Terms of Kinetic Model

term	description
$N_{Ag}(t)$	amount of Ag^+ in hydrated layer at time t (ions/unit area)
$N_B(t)$	amount of bacteria at time t (colony forming unit/mL, CFU/mL)
$[Ag^+]$	max concentration of Ag^{1+} in the hydrated layer in contact with the glass (determined from leach data)
T	thickness of the contacted hydrated layer which is calculated from the inoculum volume/6.25 cm^2
$T[Ag^+]$	max amount in the hydrated layer/cm^2
Q	rate constant controlling the release of the Ag ions from the glass into the hydrated layer; determined from leach vs time data
K_{Ag}	bacteria killing rate constant which is an adjustable parameter to fit the experimental kill vs time data
k_B	bacteria growth or death rate constant; this accounts for the bacteria continuing to grow or die naturally during the exposure time

3.5. Model Predictions. *3.5.1. Effect of Humidity.* At this point all of the factors described in the previous sections are brought to bear on the anticipated antimicrobial property of the glass surface. In other words, how the silver initially introduced into the glass ultimately can lead to antimicrobial activity and more importantly the factors that control the efficacy. The kinetic model described above allows us to incorporate the various factors in a quantitative way to the AM activity. To estimate the role of the ambient humidity, the following procedure is carried out: First, an example Ag concentration in the glass is selected which in this case will be that produced from a certain $AgNO_3$/alkali NO_3 bath and is measured by SIMS or EMP to have an x molar fraction of (Ag/total alkali). Then, the data of Figure 5 is used to determine the molar fraction of Ag^+ in solution (~hydrated layer) that can be converted to ions/unit area. This yields the value of $[Ag^+]$ in eq 6 which is defined in Table 3. Then, experimental hydrated layer thickness as a function of the relative humidity is used from Figure 3 for the values of "T". The model is then used to calculate the predicted AM efficacy as a function of the relative humidity using the numerical solution of eqs 6 and 7 with the following inputs listed below; log reduction is computed after 120 min exposure. The individual calculated fits to the experimentally measured log reduction for two humidity conditions (30% and 42% RH) and two molar fractions of Ag/total alkali (0.65 and 0.52) are listed in the following sets of Figure 6a–d. Each figure shows the values for the parameters used in the calculation.

The calculated log reduction compared to the measured AM data for *S. aureus*, using AM protocol for the four conditions, is shown below in Table 4. The parameters that are varied are the silver concentration in hydrated layer corresponding to the measured values shown in Table 2 and the thickness of the hydrated layer consistent with the humidity that is shown in Figure 3. Experimental data shows the antimicrobial efficacy of the Ag IOX samples at these relative humidity levels at 23 °C. The data shows that the log reduction increases as the % RH and as a function of the concentration of silver in the glass.

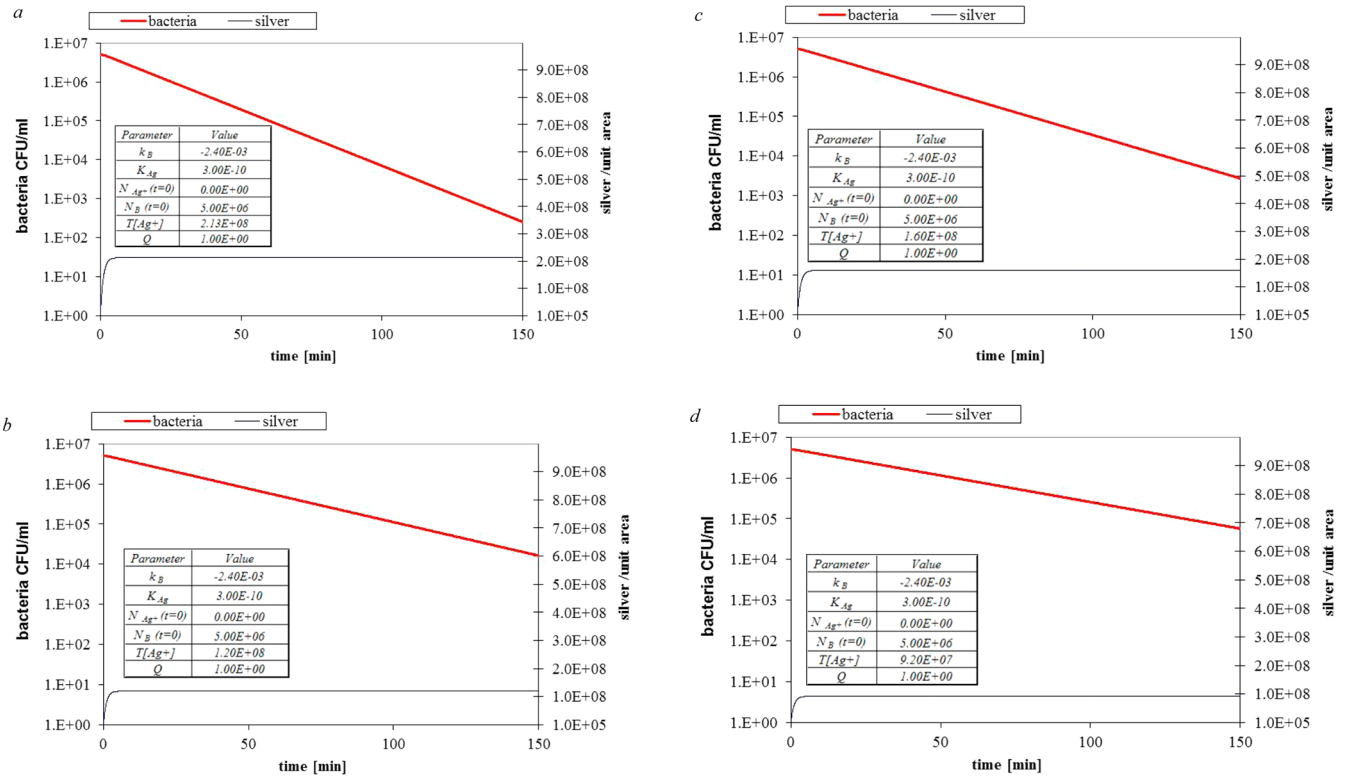

Figure 6. Examples of numerical solutions of eqs 6 and 7 for the bacteria concentration (CFU/mL) and Ag concentration in hydrated layer (silver ions/unit area) vs time for RH, molar fraction (Ag/total alkali) in glass, respectively: (a) 42%, 0.65, (b) 30%, 0.65, (c) 42%, 0.52, (d) 30%, 0.52.

DOI: 10.1021/am508159z
ACS Appl. Mater. Interfaces 2015, 7, 2195–2201

Table 4. Model and Experimental Data for Bacteria Log Reduction (Upper and Lower Limit) versus Relative Humidity and Ag Concentration in Hydrated Layer[a]

		Log reduction 42% RH		Log reduction 30% RH	
mole fraction (Ag/total alkali) in glass	Ag concentration in hydrated layer (ions/cc)	model	expt	model	expt
0.65	1.22×10^{15}	3.4	3.1−3.6	2.0	1.37−1.4
0.52	0.9×10^{15}	2.6	2.8−3.0	1.5	1.30−1.35

[a]The agreement between the model and the AM test data is quite good, indicating that the salient features of the kill phenomenon have been taken into account.

4. CONCLUSIONS

Overall, it has been shown that glasses containing Ag introduced by ion-exchange can produce a viable antimicrobial surface if care is taken to understand the physical and chemical processes which contribute to the overall antimicrobial efficacy. These various processes interact so that to find an optimum set of conditions for maximum antimicrobial efficacy, one must understand each in some detail. To that end, a model was used to show the amount of Ag that is in the glass ion exchanged from bath, and ultimately how much ends up on the surface in the hydrated layer. An explicit understanding of the role of the hydrated layer, and how it relates to the ambient and how critical it is in evaluating the specific antimicrobial test results, is discussed. It has also allowed a quantitative estimate of the log reduction as a function of the relative humidity and the Ag concentration. Finally, AM experimental results are provided that show a good correlation to the model predicted values indicating that the kinetic model has taken the necessary features into account.

■ ASSOCIATED CONTENT

Supporting Information

Details of the antimicrobial testing protocols, the bacteria used, and the log reduction calculations. This material is available free of charge via the Internet http://pubs.acs.org/.

■ AUTHOR INFORMATION

Corresponding Author

*E-mail: BorrelliNF@corning.com.

Notes

The authors declare no competing financial interest.

■ ACKNOWLEDGMENTS

Authors wish to thank a number of colleagues at Corning Incorporated; Joseph Schroeder (Glass Research) and Advanced Materials and Processing laboratory for sample preparation; Karl Koch for assistance with the kinetic model; AM assay team for AM data; Benjamin Hanson (EMP), Georgiy Guryanov (SIMS), Elzbieta Bakowska (ICP/MS) in Characterization and Materials Processing for various characterization; Tomas Seward for critical review of the paper; and Gary Calabrese, Prantik Mazumder, and Carlo Kosik-Williams for helpful discussions for the paper.

■ REFERENCES

(1) Russell, A. D.; Hugo, W. B. Antimicrobial Activity and Action of Silver. *Prog. Med. Chem.* **1994**, *31*, 351−70.

(2) Kim, J. S.; Kuk, E.; Yu, K. N.; Kim, J.-H.; Park, S. J.; Lee, H. J.; et al. Antimicrobial Effects of Silver Nanoparticles. *Nanomed.: Nanotechnol., Biol. Med.* **2007**, *3*, 95−101.

(3) Esteban-Tejada, L.; Malpartida, F.; Esteban-Cubillo, A.; Pecharroman, C.; Moya, J. S. The Antibacterial and Antifungal Activity of a Soda-Lime Glass Containing Silver Nanoparticles. *Nanotechnology.* **2009**, *20*, 85103−7.

(4) Xiu, Z.; Zhang, Q.; Puppala, H. L.; Colvin, V. L.; Alvarez, P. J. J. Negligible Particle-Specific Antibacterial Activity of Silver Nanoparticles. *Nano Lett* **2012**, *12*, 4271−5.

(5) Silver, M. K. Coordination Compounds with Antimicrobial Properties. *Appl. Organomet. Chem.* **2013**, *27*, 683−7.

(6) Reddy, P. R. S.; Rao, K. M.; Rao, K. S. V. K.; Shchipunov, Y.; Ha, C.-S. Synthesis of Alginate Based Silver Nanocomposite Hydrogels for Biomedical Applications. *Macromol. Res.* **2014**, *22*, 832−42.

(7) Lok, C.-N.; Zou, T.; Zhang, J.-J.; Lin, I.W-S.; Che, C.-M. Controlled-Release Systems for Metal-Based Nanomedicine: Encapsulated/Self-Assembled Nanoparticles of Anticancer Gold(III)/Platinum(II) Complexes and Antimicrobial Silver Nanoparticles. *Adv. Mater.* **2014**, *26*, 5550−7.

(8) Azocar, M. I.; Tamayo, L.; Vejar, N.; Gomez, G.; Zhou, X.; Thompsom, G.; et al. A Systematic Study of Antibacterial Silver Nanoparticles: Efficiency, Enhanced Permeability, and Cytotoxic Effects. *J. Nanopart. Res.* **2014**, *16*, 1−9.

(9) Verne, E.; Nunzio, S. D.; Bosetti, M.; Appendino, P.; Brovarone, C. V.; Maina, G.; et al. Surface Characterization of Silver Doped Bioactive Glasses. *Biomaterials* **2005**, *26*, 5111−9.

(10) Thurman, R. B.; Gerba, C. P. The Molecular Mechanisms of Copper and Silver Ion Disinfection of Bacteria and Viruses. *Crit. Rev. Environ. Control* **1989**, *18*, 295−315.

(11) Kosik-Williams, C.; Borrelli, N.; Senaratne, W.; Wei, Y.; Petzold, O. Touchscreen Surface Warfare—Physics and Chemistry of Antimicrobial Behavior of Ion-Exchanged Silver in Glass. *Am. Ceram. Soc. Bull.* **2014**, *93*, 20−4.

(12) Schulze, G. Experiments Relating to the Diffusion of Silver into Glass. *Ann. Phys.* **1913**, *40*, 335−67.

(13) Borrelli N., Morse D., Senaratne W., Wei Y., Verrier F. Coated, Antimicrobial, Chemically Strengthened Glass and Methods of Making. U.S. Patent 8753744, 2014.

(14) Garfinkel, H. H. Ion-Exchange Equilibria between Glass and Molten Salts. *J. Phys. Chem.* **1968**, *78*, 4175−81.

(15) Araujo, R. J.; Litkitvanichkul, S.; Allen, D. C. Ion Exchange Equilibria between Glass and Molten Salts. *J. Non-Cryst. Solids* **2003**, *318*, 262−7.

(16) Kistler, S. S. Stresses in Glass Produced by Nonuniform Exchange of Monovalent Ions. *J. Am. Ceram. Soc.* **1962**, *45*, 59−68.

(17) Paje, S. E.; Garcia, M. A.; Llopis, J.; Villegas, M. A. Optical Spectroscopy of Silver Ion-Exchanged As-Doped Glass. *J. Non-Cryst. Solids* **2003**, *318*, 239−47.

(18) Paje, S. E.; Garcia, M. A.; Villegas, M. A.; Llopis, J. Optical Properties of Silver Ion-Exchanged Antimony Doped Glass. *J. Non-Cryst. Solids* **2000**, *278*, 128−36.

(19) Araujo, R. Colorless Glasses Containing Ion Exchanged Silver. *Appl. Opt.* **1992**, *31*, 5221−4.

(20) JIS Z2801 Antibacterial Products. Test for Antibacterial Activity and Efficacy Japanese Industry Standard, 2010.

(21) Test Method for Efficacy of Copper Alloy Surfaces as a Sanitizer. Environmental Protection Agency, 2010.

(22) Santo, C. E.; Lam, E. W. Bacterial Killing by Dry Metallic Copper Surfaces. *Appl. Environ. Microbiol.* **2011**, 794−802.

(23) Iler, R. K. *The Chemistry of Silica*; John Wiley & Sons: New York, 1979.

DOI: 10.1021/am508159z
ACS Appl. Mater. Interfaces 2015, 7, 2195−2201

(24) Zhuravlev, L. T. The Surface Chemistry of Amorphous Silica. Zhuravlev Model. *Colloids Surf., A* **2000**, *173*, 1−38.
(25) Saliba, N. A.; Yang, H.; Finlayson-Pitts, B. J. Reaction of Gaseous Nitric Oxide with Nitric Acid on Silica Surfaces in the Presence of Water at Room Temperature. *J. Phys. Chem. A* **2000**, *105*, 10339−46.

DOI: 10.1021/am508159z
ACS Appl. Mater. Interfaces 2015, 7, 2195−2201